International Journal of Navigation and Port Research
Vol.31, No.7 pp. 589~595, 2007 (ISSN-1598-5725)

Numerical analysis on Deformation of Seabed Structures with various size materials by DEM

Mi-Kum Kim · †Chang-Je Kim***

** Department of Civil Engineering, Tottori University, Tottori, 680-8552, Japan*
*** Division of Navigation System Engineering, Korea Maritime University, Busan 606-791, Republic of Korea*

Abstract : *In the majority of previous studies on deformation of seabed structures using DEM, elements of structures have been assumed that it is composed with uniform materials or received fixed wave force, despite that actual submerged structures are composed with various size materials and influenced by complicated fluid field. The goal of this study is to develop a new model for analysis of seabed structure deformation using discontinuous structures composed with various size materials. As the first phase, a model using DEM and VOF, which can compute the deformation of submerged structures composed with various size materials, such as rubble mound structures , is proposed. A model test is carried out and then the validity of the model is discussed.*

Key words : *Distinct Element Method; Rubble mound; Submerged breakwater; VOF; Morison model; Rubble mound structure;*

1. Introduction

In numerical analysis on deformation of submerged structures such as rubble mounds, cavern formation process in sandy beach, and seabed liquefaction, Distinct Element Method (DEM), which has been proposed by Cundall, P. A. (1971), is recently used well. DEM has the essential applicability for analysis of fissured rock structures and discontinuous structures on seabed. However, in the majority of DEM analysis of the previous studies on submerged structures, elements of structures were assumed that it is constructed with uniform materials (Araki et al., 2001; Araki et al., 2003), despite that actual submerged structures are constructed with various size materials. Therefore, the structures were divided into same size elements and analyzed. Furthermore, it was assumed that waves acting on the structures are dealt with by simple cyclic condition for the stable computation, and the wave forces were acted on the just surface layer for simplicity. The results of analysis with assumed seabed or submerged structures are significantly different from those of actual states.

And in case of analysis on deformation of submerged structure caused by wave force, though the interaction of wave field and sectional deformation of structure is an important factor, previous studies rarely considered it.

The goal of this study is to develop a new model for analysis of seabed structure deformation using discontinuous structures with various size materials. As the first phase, we propose a model that the deformation of the submerged rubble mound structures composed with various size materials can be computed.

The proposed model in this study has two sub-modules. One is wave computation module by CADMAS-SURF (Coastal Development Institute of Technology, 2001) based on VOF (Hirt and Nichols, 1981) and SMAC method. And the other is structure computation module by DEM. In the wave module, Morison model is adapted to determine wave forces.

In this study, we try to compute the deformation of the rubble mound structure with various size materials on seabed and the deformation of seabed. The wave field to a porous mound structure is computed by CADMAS-SURF. And the deformation of structure is computed using DEM module. The wave forces are acted not just surface area, but those are acted into all elements in the structure, and then the behaviors of all elements are traced. Furthermore, interaction of wave and sectional deformation of structures is considered and the influences due to the configuration of coefficients in analysis on the deformation of the submerged structure are investigated.

2. Wave Analysis

2.1 Reproduction of wave field

In this study, for computation of wave field, CADMAS-SURF is accepted. CADMAS-SURF is useful tool to

* ddochi-77@hanmail.net 051)410-4226
† Corresponding Author : chang-je kim, kimc@hhu.ac.kr (051)410-4226

compute the time and space variations of water free surface based on VOF and SMAC method. Furthermore, CADMAS-SURF can be applied on the analysis of special topographical feature such as sloping surface of seabed and porous structures. The governing equations of CADMAS-SURF, which are expanded on the basis of porous model with the Navier-Stokes equation and the continuity equation for 2-D incompressible inviscid fluid, are given as follows:

$$\frac{\partial \gamma_x u}{\partial x}+\frac{\partial \gamma_z w}{\partial z}=S_\rho \tag{1}$$

$$\lambda_v\frac{\partial u}{\partial t}+\frac{\partial \lambda_x uu}{\partial x}+\frac{\partial \lambda_z uu}{\partial z}=-\frac{\gamma_v}{\rho}\frac{\partial p}{\partial x}+\frac{\partial}{\partial x}\left\{\gamma_x \nu_e\left(2\frac{\partial u}{\partial x}\right)\right\} +\frac{\partial}{\partial z}\left\{\gamma_z \nu_e\left(\frac{\partial u}{\partial z}+\frac{\partial w}{\partial x}\right)\right\}-D_x u+S_u-R_x \tag{2}$$

$$\lambda_v\frac{\partial w}{\partial t}+\frac{\partial \lambda_x uw}{\partial x}+\frac{\partial \lambda_z ww}{\partial z}=-\frac{\gamma_v}{\rho}\frac{\partial p}{\partial z}+\frac{\partial}{\partial x}\left\{\gamma_x \nu_e\left(2\frac{\partial w}{\partial x}+\frac{\partial u}{\partial z}\right)\right\} +\frac{\partial}{\partial z}\left\{\gamma_z \nu_e\left(2\frac{\partial w}{\partial z}\right)\right\}-D_z w+S_w-R_z-\gamma_v g \tag{3}$$

where, t is time, x and z are the horizontal and the vertical, u and w are the velocities of horizontal and vertical of the flow, ρ is the density, p is the pressure, ν_e is sum of the molecular dynamic viscosity and the eddy dynamic viscosity, g is the gravity acceleration, γ_v is the porosity, γ_x and γ_z are the area transmittances of horizontal and vertical, $\lambda_v=\gamma_v+(1-\gamma_v)C_M$, $\lambda_x=\gamma_x+(1-\gamma_x)C_M$, $\lambda_z=\gamma_z+(1-\gamma_z)C_M$, C_M is inertia coefficient. And D_x and D_z are coefficients on damping area of energy, S_ρ , S_u and S_w are the source terms for wave source. And resistance from porous structure, R_x and R_z, are expressed as follows:

$$R_x=\frac{1}{2}\frac{C_D}{\Delta x}(1-\gamma_x)u\sqrt{u^2+w^2} \tag{4}$$

$$R_z=\frac{1}{2}\frac{C_D}{\Delta z}(1-\gamma_z)w\sqrt{u^2+w^2} \tag{5}$$

where, C_D is the drag coefficient, Δx and Δz are the cell intervals of direction x and z .

Advection equation of F, relational algebra of VOF, based on porous model is given as follow:

$$\gamma_v\frac{\partial F}{\partial t}+\frac{\partial \gamma_r uF}{\partial x}+\frac{\partial \gamma_z wF}{\partial z}=0 \tag{6}$$

2.2 Computation of wave force

Wave forces to elements are calculated as follows:

$$F_d=\frac{1}{2}\rho A C_D' U_D|U_D| \tag{7}$$

$$F_i=\rho V C_M'\dot{U}_D \tag{8}$$

$$F_l=\frac{1}{2}\rho A C_L' U_D^2 \tag{9}$$

where, F_d is the drag force, F_i is the inertia force, F_l is the upward force, ρ is the density of a fluid, A is the area of projection, U_D is the relative velocity vector of element and fluid, V is the volume of element, C_M' is the inertia coefficient, $\dot{U}_D$ is the acceleration vector and C_L' is the lift coefficient. In this study, acceleration vector of fluid is used for the acceleration vector .

3. Structure Analysis

Described model herein is a two-dimensional model (Kiyama et al., 1988). The driving forces are gravity and wave force. The solution algorithms are briefly described in following section.

3.1 Outline of DEM

In DEM analysis, rocks are treated as the rigid and elastic body, and non-elastic property of rock is expressed by inserted elastic spring with the contact coefficient K and cohesion dashpot with the damping coefficient η into contact point between rocks. Then, the equations of translation motion X and rotary motion ϕ of the one rock with mass m and the inertial moment I are expressed as follows:

$$m\ddot{X}+\eta\dot{X}+KX=0 \tag{10}$$

$$I\ddot{\phi}+\eta r^2\dot{\phi}+Kr^2\phi=0 \tag{11}$$

where, X denotes displacement with vectorial property and r is radius of rock.

These equations denote the diminish violation. And analysis of the rock motion from movement to stillness is possible by computing the equations of motion for all rocks. But, generally, it is difficult to solve Eq. 10 and Eq. 11, simultaneously, because a rock contacts with several rocks and the unknown displacement, Δx, Δz and ϕ are contained implicitly. Therefore Cundall proposed the progressional solution method by differential approximation using time step Δt in Eq. 10 and Eq. 11 and by

approximation of the equation which the unknown displacements are contained explicitly. For example, Eq. 10 is represented as follow.

$$m[\ddot{X}]_t = -\eta[\dot{X}]_{t-\Delta t} - K[X]_{t-\Delta t} \tag{12}$$

And then the equation is calculated by the assumption that new acceleration $[\ddot{X}]_t$, which new displacement $[X]_t$ is calculated by integral of $[\ddot{X}]_t$, is the explicit relational algebra of force at contact on the basis of displacement $[X]_{t-\Delta t}$ at the last step.

3.2 Improvement of efficiency for contact judgment

The contact judgment is improved in order to reduce the run-time of computation. First, the whole calculation area is divided into equal small section, that is, the ranges of $0 \le x \le a$ and $0 \le z \le b$ are divided into m and n sections, respectively. Then, the section number of center $G(x, z)$ of element is investigated using the following equation.

$$N = m \cdot FIX\left[\frac{z_i}{b/n}\right] + FIX\left[\frac{x_i}{a/m}\right] + 1 \tag{13}$$

where, FIX denotes to make the integer by cutting the below of decimal point. By this calculation, the section number of i is decided. The section containing j with the possibility on contacting to i is restricted with one section containing j and eight adjacent sections. Then, when the detailed contact judgment for elements $j(\neq i)$ in nine sections is carried out, simple and speedy calculation is realized.

3.3 Coupling of DEM and VOF

Coupling of DEM and VOF is accomplished as Eq.(14)~ Eq.(16) by adding the calculated wave force into the equations of motion of DEM.

$$(M_i + M_i')\ddot{x} = \sum_j [F_x]_{ij} + [f_x]_i \tag{14}$$

$$(M_i + M_i')\ddot{z} = \sum_j [F_z]_{ij} + [f_z]_i + v_i(\rho_p - \rho)g \tag{15}$$

$$(\phi_i + \phi_i')\ddot{\omega} = \sum_j [M_x]_{ij} \tag{16}$$

where, M_i and M_i' are mass and additional mass of element i, $\ddot{x}$ and $\ddot{z}$ are acceleration components to direction x and z, $[F_x]_{ij}$ and $[F_z]_{ij}$ are contact forces from contacted element j, $[f_x]_i$and $[f_z]_i$ are wave forces. And ϕ_i and ϕ_i' are the moment of inertia and the additional moment of inertia, v_i is volume of element, ρ_p is density of element, $\ddot{\omega}$ is angular acceleration to direction of each axis, $[M]_{ij}$ is moment to around each axis.

4. Application To Analysis

4.1 Making the incipient mound

In this study, a model test associated with deformation of submerged structure due to wave action is carried out. And to investigate difference by composition of materials, two models are used. One is model composed of various size materials. The other is model composed of uniform size materials. Computation area and mound model set-up are depicted in Fig. 1. And the initial shape of mound with various sizes is made as shown in Fig. 2. In case of model composed of various size materials, the mound is composed by 1500 elements with a radius of 2cm, 200 elements with a radius of 4cm and 300 elements with a radius of 5cm. Making process of initial mound is simplified as follow. First, the seabed with uniform size elements with a radius of 2cm is composed. Then, the mound using elements with a radius of 4cm, 5cm and 4.5cm is made by free fall on the seabed. Although actual seabed is composed with smaller elements, elements with a radius of 2cm are used for simplify of computation.

And in case of model composed of uniform size materials, the mound and the seabed are composed by 500 elements with a radius of 4.5cm and 1500 elements with a radius of 2.0cm, respectively, as shown in Fig. 3.

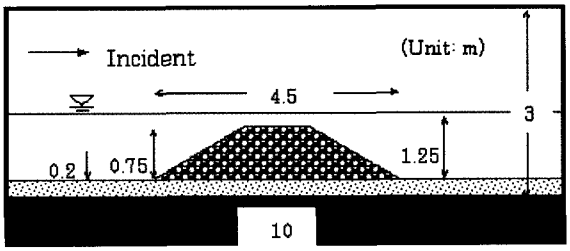

Fig. 1 Computation area and model set-up

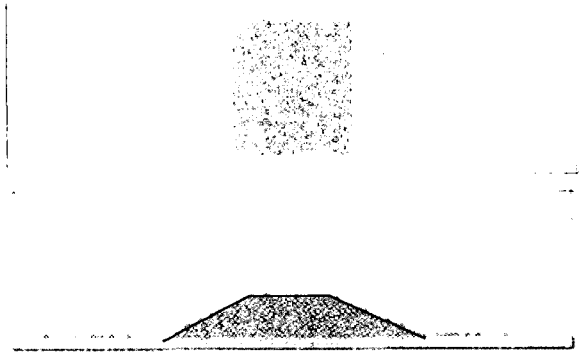

Fig. 2 Making process of initial mound and result with various size materials

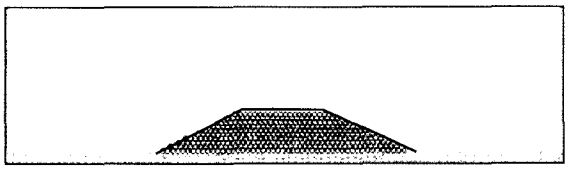

Fig. 3 Initial mound with uniform size materials

4.2 Analysis on Wave

In wave computation module, the CADMAS-SURF is adapted, and incipient mound model by DEM computation is used to compute the porous structure. The porosity of porous structure is set 0.4 according to the previous study (Maeno et al., 2006). The computations are carried out under regular wave with the wave height of 0.3m and the period of 2.0s. And time interval Δt is 0.01s.

The surface elevation, water particle velocity vector in wave field and computation points of wave forces are shown in Fig. 4. And, the time variations of wave force computed by Morison module with wave velocities at Pts.1~7 are shown in Fig. 5. In wave analysis, for the value of C_M and C_D , 1.5 and 0.5 are adapted, according to the formulary on hydraulics (Japan society of civil engineers, 1971).

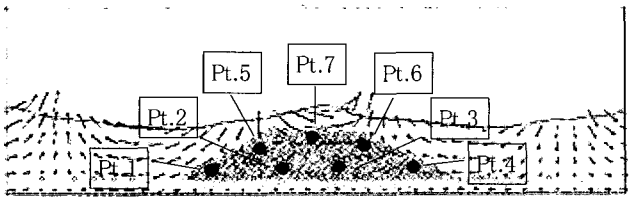

Fig. 4 Wave profile in object area and selected points

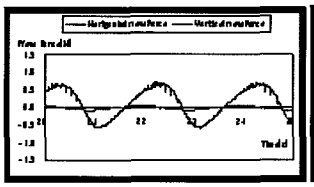

Fig. 5(a) Wave forces at Pt.1

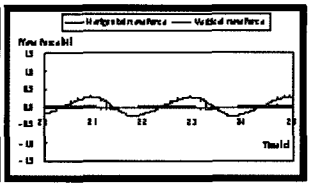

Fig. 5(b) Wave forces at Pt.2

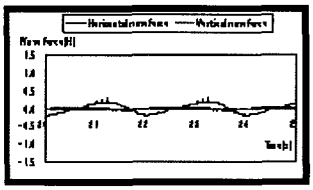

Fig. 5(c) Wave forces at Pt.3

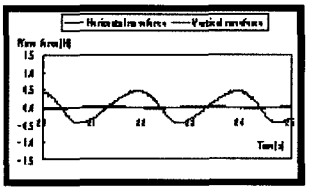

Fig. 5(d) Wave forces at Pt. 4

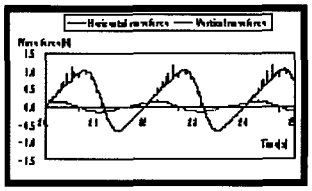

Fig. 5(e) Wave forces at Pt.5

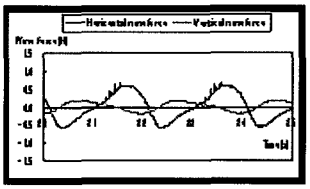

Fig. 5(f) Wave forces at Pt.6

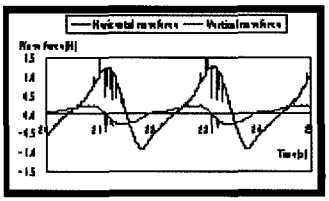

Fig. 5(g) Wave forces at Pt.7

4.3 Analysis on structure deformation

Analysis on mound deformation is performed against the submerged breakwater model. In this case, for simplify of computation, the wave forces are inputted under simplify procedure that one cycle of wave force is divided into some sections and represented by the average of that section. Furthermore, the seabed structure deformation is computed simultaneously, and then the interaction of seabed and mound is taken account.

Generally, the coefficients between elements such as the contact force and the damping coefficient are determined so as not inordinate repulsing and sinking. Therefore, the coefficients are determined by the method of trial and error.

Fig. 6 shows computed result with mound composed of uniform size material and Fig. 7(a)-(d) show computed results with mound composed of various size materials under the conditions as shown in Table 1.

Firstly, to investigate difference of computed results using two models composed of uniform size materials and various size materials, Fig. 6 and Fig. 7(a) are compared. In this case, conditions in Case 1 are used. From the result in Fig. 6, it is found that movements of elements are restricted and change in the height of the crest by compaction is greatly smaller than that in Fig. 7(a). Because, in case of mound composed of uniform size material, there is little space between materials. Therefore the behavior is restricted and compaction by wave action is not expressed, despite that actual submerged mound structures are compacted by wave action.

Secondly, in order to investigate the influence of computation time on the deformation of the model mound, the computed result after 15s in Fig. 7(a) is compared with that after 30s in Fig. 7(b). From Fig. 7(a), the elements moved onshore and offshore directions and then scattered at 15 s after wave action. From Fig. 7(b), it is found that height of crest caused by compaction is higher than that of Fig. 7(a). But the remarkable deformation to horizontal direction is not shown.

Thirdly, the difference by the contact stiffness was investigated. From the computed result in Fig. 7(c), it is found that the seabed elements moved and mixed with mound elements and mound elements moved to onshore

direction. The change of the mound shape is slightly lager than that of Case 1. The computed result in Case 3 indicates that the contact stiffness plays an important role in the deformation of mound structures. By inputting the large contact stiffness, strong contact force is generated and movements of elements are activated.

Finally, the difference of deformation caused by the friction coefficient is examined. From Fig. 7(d), it is found that the movements of the elements to horizontal direction are a little restricted. But, remarkable difference is not shown.

Table 1 Input data

	Δt (s)	Time(s)	Contact Stiffness (N/m)	Friction angle (degree)
Case 1	1×10^{-4}	15	1×10^{4}	25
Case 2	1×10^{-4}	30	1×10^{4}	25
Case 3	5×10^{-5}	15	1×10^{5}	25
Case 4	1×10^{-4}	15	1×10^{4}	35

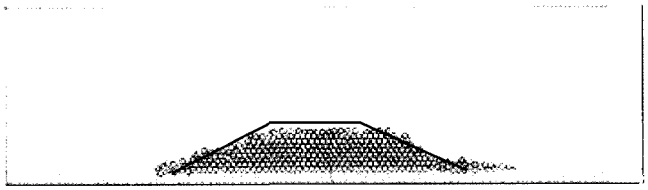

Fig. 6 Sectional deformation of mound by wave force with regular size materials (case 1)

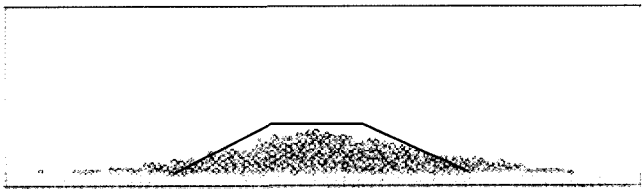

Fig. 7(a) Sectional deformation of mound by wave force with various size materials (case 1)

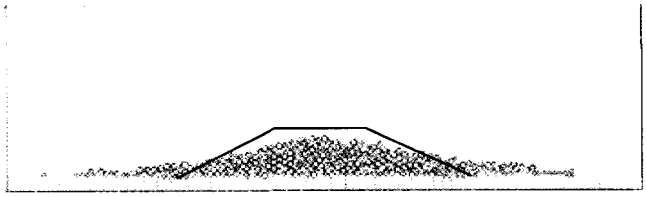

Fig. 7(b) Sectional deformation of mound by wave force with various size materials (case 2)

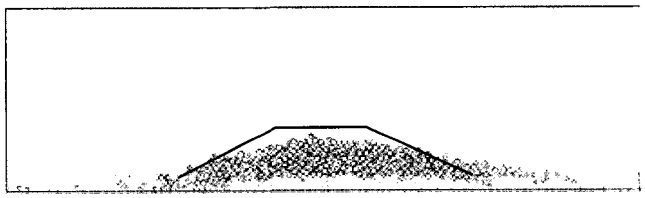

Fig. 7(c) Sectional deformation of mound by wave force with various size materials (case 3)

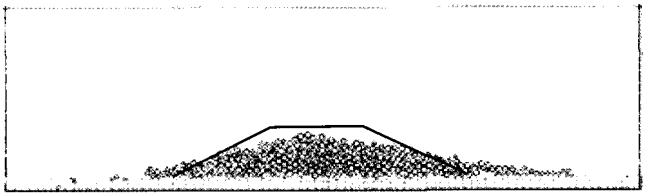

Fig. 7(d) Sectional deformation of mound by wave force with various size material (case 4)

4.4 Analysis on interaction of deformation and wave

In this section, in order to investigate the interaction of wave and sectional deformation, the second analysis, which means feedback to wave computation, is performed using the deformed mound by wave action in the first step. Although it is desirable that consideration of the interaction between wave field and deformation of the structure is performed every time step and that was performed in few case (Itoh et al., 2001), in case of computation with many elements, that is difficult from the viewpoint of calculation time and stability. Therefore, in this study, time interval of 15s per step is adopted for efficiency and stability of calculation.

The wave conditions in section 4.2 are used. In the second step, for the porosity of the lower part of porous structure, 0.37 is inputted according the previous study (Maeno et al., 2006).

A fragment of result of wave computation is expressed in Fig. 8 and the time variations of wave forces at each point are expressed in Fig. 9. Remarkable differences of wave are not shown. Analysis on mound deformation was accomplished with deformed mound model, as shown in Fig. 7(a), and calculated wave force by Morison model. As ever section 4.3,inputted wave force is simplified. Conditions of DEM computation in this section are equal to Case 1. The result of analysis is shown in Fig. 10. From comparing with Fig 7(a) it is found that the height of crest caused by wave action is lower than Fig. 7(a). And from comparing with Fig. 7(b), it is found that tops of on and offshore side of mound are more depressed than that of Fig. 7(b). This result indicates that to consider the interaction between wave and deformation is important.

Furthermore, result of computation at second step under condition of case 3 is shown in Fig. 11. From this figure, it is found that although the change of the mound at second step is small, the mound is more depressed.

The overall results of computations are shown in Table 2. By numerical comparison, differences of computation results under the various conditions as remarked above are found clearly.

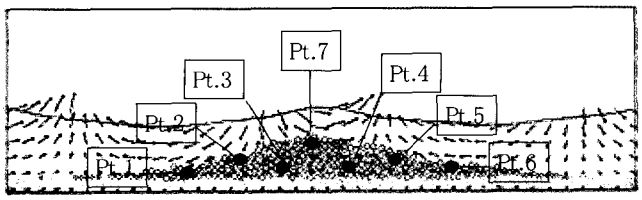

Fig. 8 Wave profile in object area and selected points at second step

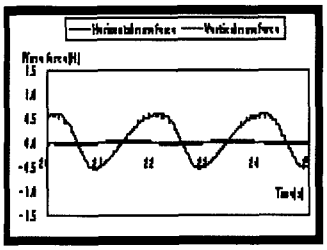

Fig. 9(a) Wave forces at Pt.1

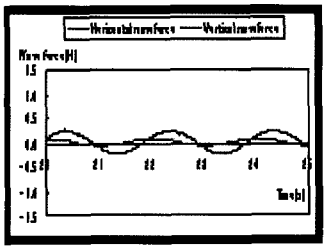

Fig. 9(b) Wave forces at Pt.2

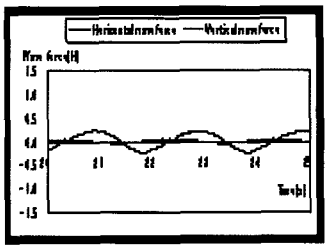

Fig. 9(c) Wave forces at Pt.3

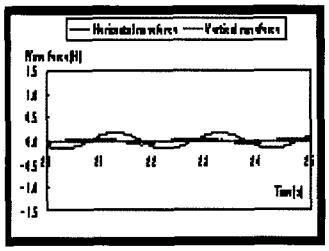

Fig. 9(d) Wave forces at Pt.4

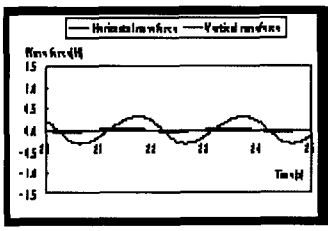

Fig. 9(e) Wave forces at Pt.5

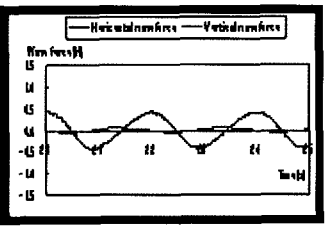

Fig. 9(f) Wave forces at Pt.6

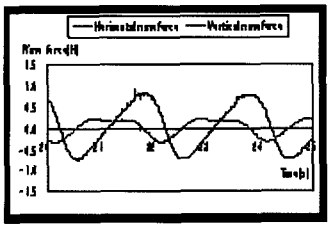

Fig. 9(g) Wave forces at Pt.7

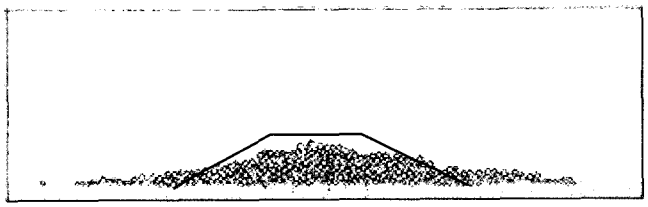

Fig. 10 Sectional deformation of mound by two steps with various size materials (Case 1)

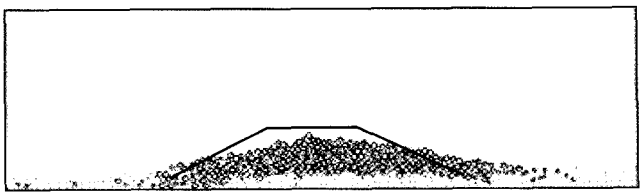

Fig. 11 Sectional deformation of mound by two steps with various size materials (Case 3)

Table 2 Results of computations

	The height of crest (cm)	Elements in outer parts of mound (ea)	
		offshore side	onshore side
Fig. 6	7. 6	8	12
Fig. 7(a)	8. 7	26	31
Fig. 7(b)	16. 7	32	34
Fig. 7(c)	12. 3	17	33
Fig. 7(d)	10. 9	17	31
Fig. 10	13. 5	30	35
Fig. 11	12. 9	18	33

5. Conclusions

In this study, analysis on mound deformation caused by wave force was performed by coupling CADMAS-SURF and DEM. Wave was calculated by CADMAS-SURF against incipient mound by DEM analysis and wave force was calculated by wave velocities and Morison model. And deformation of mound was calculated by DEM. As a result, wave forces in mound were reflected comparatively in detail and the discrepancy of sectional deformation which caused by setting of coefficients were expressed. And influence of interaction between wave and sectional deformation was expressed by the separated analysis into two steps. But, to reflect the wave forces into mound at real time without simplify processing and to consider the sequential interaction of sectional deformation and wave were not accomplished in here.

Hence, the model in this study is required some improvements such as to reflect the actual wave force into structure and to consider the sequential interaction of deformation and wave. And to consider the random properties of materials of structure is required, because behavior of element is influenced by random properties of material such as contact force, shapes and small unevenness of surface and so on. By these improvements, more satisfactory analysis on deformation of structure is expected.

References

[1] Araki, S., Kotake, Y. Kanazawa, T., Matsumura, A., and Deguchi, I. (2001), "Numerical simulation of deformation of rubble mound seawall with VOF and DEM", Proceedings of coastal engineering, JSCE, Vol. 48, pp.931-935.

[2] Araki, S. Yanagihara, T., and Deguchi, I. (2003). "Numerical simulation on 3-dimensional deformation of submerged breakwater with discrete element method", Proceedings of coastal engineering, JSCE, Vol. 50, pp.831-835.

[3] Coastal Development Institute of Technology (2001), "Research and development of CADMAS-SURF", No.12.

[4] Cundall, P. A. (1971), "A computer model for simulating progressive, large-scale movements in blocky rock systems", Symposium on rock mechanics, Nancy, Vol.2, pp.129-136.

[5] Hirt, C. W. and Nichols, B. D. (1981), "Volume of fluid method for the dynamics of free boundaries", J. Comp. Phys., Vol.39, pp.201-225.

[6] Itoh, K., Higuchi, Y., Toue, T., and Katsui, H. (2001). "DEM simulation of submerged breakwater deformation in consideration for randomness of rubbles", Proceedings of coastal engineering, JSCE, Vol. 48, pp.806-810.

[7] Japan Society of Civil Engineers. (1971), Formulary on hydraulics, pp. 523.

[8] Kiyama, H., Fujimura, H., and Nishimura, T. (1988), "Theoretical analysis of Fenner-Pacher type characteristic curves for tunneling by DEM", Journal of geotechnical engineering, 394/2-9, pp. 37-44.

[9] Maeno, S., Ogawa, M., and Bierawski, L. G. (2006), "Analysis on deformation of the permeable submerged breakwater by coupling of VOF, DEM and FEM", Annual conference of Coastal Engineering, JSCE, Vol. 53, pp.886-890.

Received 19 June 2007
Accepted 28 September 2007